Approximation of Wave Action Conservation in Vertically Sheared Mean Flows

Saeideh Banihashemi and James T. Kirby

Center for Applied Coastal Research, Department of Civil and Environmental Engineering, University of Delaware, Newark, DE 19716 USA
Corresponding author: Email address:bhashemi@udel.edu

Abstract

We develop asymptotic expressions for wave action density and action flux, using an extension of Kirby & Chen (1989)'s perturbation solution for weakly-sheared currents allowing for a basic flow with Froude number $F = U/\sqrt{gh} = O(1)$ but with weak vertical shear. The accuracy of the expressions for action density and flux are established by comparison to analytic results for a current with constant shear, and to numerical results for a field case involving a buoyant ebb-tidal plume with strong vertical shear and for a case involving a numerically determined profile for a wind-driven current. We compare our results to those from recent work of Quinn *et al.* (2017), and find unresolved discrepancies in that prior work. We provide additional suggestions for efficiently implementing the required extensions in coupled wave/circulation models using a Taylor series expansion based on conditions at peak frequency and direction. These results generalize the previous work of Banihashemi *et al.* (2017) to motions in two horizontal dimensions, and cover the determination of the wave action.

Keywords: wave-current interaction, wave action conservation, ocean

models, waves over sheared currents

---

1. Introduction

Significant advances have been made in the numerical modeling of wave-current interaction in recent decades. An important component in these advances has been the recognition of wave action as the fundamental conserved quantity expressing the wave-averaged energy of a slowly-varying wave train. The simplest description is typically based on the underlying dynamics for monochromatic waves, governed by the wave action balance of Bretherton & Garrett (1968) and given by

$$\mathcal{N}_{,t} + \nabla_h \cdot \boldsymbol{\mathcal{F}} = 0 \tag{1}$$

where subscripted commas denote partial differentiation. For the case of depth uniform mean current $\mathbf{U}$, action density $\mathcal{N} = E/\sigma$ and action flux $\boldsymbol{\mathcal{F}} = \mathcal{N}\mathbf{c}_{ga}$, where E is energy density, $\sigma = \omega - \mathbf{k}\cdot\mathbf{U} = \sqrt{gk\tanh kh}$ is intrinsic frequency, h and $k = |\mathbf{k}|$ are depth and wavenumber, and $\mathbf{c}_{ga} = \omega_{,\mathbf{k}} = \sigma_{,\mathbf{k}} + \mathbf{U}$ is the absolute group velocity vector in stationary coordinates.

Phase-averaged spectral wave models typically calculate wave properties based on the linear theory for waves superposed on depth-uniform currents. However, currents in the field are occasionally strongly sheared over the vertical, leading to the need for a treatment of the rotationality or shear in the flow field. An approximate treatment for the effect of current shear may be based on a perturbation approach that has been developed through a sequence of papers (Stewart & Joy, 1974; Skop, 1987; Kirby & Chen, 1989;

Ellingsen & Li, 2017), with Kirby & Chen (1989, hereafter referred to as KC89) providing a solution to second order for the finite depth case for currents that are assumed to deviate only weakly from depth-uniformity.

The main utility of the approximate solution has been the specification of a depth-weighted current $\tilde{\mathbf{U}}$, specified by Skop (1987) and KC89 and given by (12) below, as a representative depth-uniform current for determining intrinsic frequency and action density in spectral wave models (van der Westhuysen & Lesser, 2007; Ardhuin *et al.*, 2008). As pointed out in the original study of KC89 and recently elaborated on by Banihashemi *et al.* (2017, hereafter BKD17), the depth weighted current $\tilde{U}$ does not represent a consistent approximation for the current contribution to the group velocity $\mathbf{c}_{ga}$ at leading order. BKD17 demonstrate the inappropriateness of the use of the weighted current $\tilde{\mathbf{U}}$ as the current speed in the expression for absolute group velocity, and establish the accuracy of the alternate value $\hat{\mathbf{U}}$ which follows naturally from consideration of the dependence of $\tilde{\mathbf{U}}$ on wavenumber k when differentiating the dispersion relation to get group velocity. The accuracy of this result provides a target for determining appropriate expressions for the group velocity for use in estimating wave action flux.

Models for spectral wave conditions more commonly solve for $\mathcal{N}(\mathbf{x}, t, \sigma, \theta)$ using a spectral action balance equation, which, for Cartesian coordinates, is given by (Hasselmann, 1973)

$$\mathcal{N}_{,t} + \nabla_h \cdot (\mathcal{N}\mathbf{c}_{ga}) + (c_\sigma \mathcal{N})_{,\sigma} + (c_\theta \mathcal{N})_{,\theta} = \frac{S}{\sigma} \tag{2}$$

where the third and forth terms represent transport in spectral space (σ, θ).

Expressions for these propagation speeds are taken from linear wave theory (Whitham, 1974; Dingemans, 1997) for waves superimposed on depth-uniform currents. The right hand side of the equation represents source and sink terms associated with wave generation, dissipation and nonlinear wave-wave interactions. The introduction to each source term included in SWAN, for example, can be found in Booij *et al.* (1999). In applications using wave models which take as input a single Eulerian current vector at each grid point from the circulation model, this approach, based on a wavenumber-dependent current speed, is often simplified by using the current value at the peak wave frequency or wavenumber, $\tilde{U}(\mathbf{k}^p)$ (for example, Elias *et al.*, 2012), or at some weighted-average wavenumber value. BKD17 further examine the effect of using either the correct or incorrect estimate of the current speed evaluated only at the spectral peak frequency. The study suggested an alternate strategy, involving a Taylor series expansion of the depth-weighted current about the peak frequency, which significantly extends the range of accuracy of current information available to the wave model with minimal additional transfer of data between wave and circulation models.

In this study, the change in the estimate of action density and action flux due to current shear is investigated, using asymptotic approximations of the Voronovich (1976) action balance equation obtained using a strong-current extension of the KC89 perturbation solution. In section 2, the problem for a linear wave in a horizontally-uniform domain with arbitrary current $\mathbf{U}(z)$ is established. In section 3 and Appendix A, KC89's perturbation solution for weakly-sheared currents is modified to allow for steady currents which are strong and oriented at arbitrary angles to the wave propagation direction.

Approximate expressions for the wave action density and action flux are then developed following a procedure described in Appendix B. The approach is similar to that of Quinn *et al.* (2017), although our results differ significantly. In section 4, we evaluate the approximations for the analytic case of a wave on a current with constant vorticity, and establish the consistency of the expressions for action and action flux derived from the perturbation solution of KC89. Section 5 considers an application to a field case involving a strongly sheared vertical profile measured in the Mouth of the Columbia River (Kilcher & Nash, 2010). In Section 6, we extend the proposed Taylor series expansion of the expressions for the wavenumber-dependent approximations about the reference value at the peak frequency, originally presented in BKD17, to include wave directionality and the variation in intrinsic frequency appearing in the denominator of the action density. The differences between our results and those of Quinn *et al.* (2017) are discussed in section 7, along with suggestions for further work. A Supplement provides a number of plots comparing action density and flux estimates based on the usual depth-uniform current expressions and using the surface or depth-averaged currents as the representative values.

2. General theory

We consider the linearized problem for periodic surface waves in an incompressible, inviscid fluid, with wave number $\mathbf{k}$ and phase velocity $\mathbf{c}_a = (\omega/k)\hat{\mathbf{k}}$, propagating on a stream of velocity $\mathbf{U}(z)$ in finite water depth h. Here, ω denotes the absolute wave frequency in a stationary frame of reference, which also fixes the value of $\mathbf{U}(z)$. A unit vector pointing in the direction of wave propagation is defined as $\hat{\mathbf{k}} = \mathbf{k}/k$. The problem is formulated in terms of the vertical component of the wave orbital velocity, written in complex form as

$$w(\mathbf{x}, z, t) = \frac{w(z)}{2} \mathrm{e}^{i(\mathbf{k}\cdot\mathbf{x}-\omega t)} + c.c. \tag{3}$$

where $c.c$ denotes the complex conjugate. The problem for the vertical structure of plane waves in a spatially uniform domain is then given by an extension of the Rayleigh equation to allow for an oblique angle between wave and current direction as well as possible rotation of the current vector over depth,

$$\sigma(z)(w_{,zz} - k^2 w) = \sigma_{,zz}(z) w; \quad -h \leq z \leq 0 \tag{4a}$$

$$\sigma^2(0) w_{,z}(0) - [g k^2 + \sigma(0)\sigma_{,z}(0)] w(0) = 0 \tag{4b}$$

$$w(-h) = 0 \tag{4c}$$

where g is the gravitational constant. The quantity $\sigma(z) = \omega - \mathbf{k} \cdot \mathbf{U}(z)$ represents a depth-varying relative frequency. We subsequently denote the values of current $\mathbf{U}(0)$ and intrinsic frequency $\sigma(0)$ at the mean surface $z = 0$ by $\mathbf{U}_s$ and σ_s, respectively. The amplitude of w may be related to surface displacement amplitude a through the kinematic surface boundary condition linearized w/r the fluctuating motion, given by

$$\eta_{,t} + \mathbf{U}_s \cdot \nabla_h \eta = w(0) \tag{5}$$

with η given by

$$\eta(\mathbf{x},t) = \frac{a}{2}\mathrm{e}^{i(\mathbf{k}\cdot\mathbf{x}-\omega t)} + c.c, \tag{6}$$

leading to the relation $w(0) = -i\sigma_s a$. This result can be extended to cover the full water depth by introducing a dimensionless shape function $f(z)$ according to

$$w(z) = -i\sigma_s a f(z); \quad f(-h) = 0, \quad f(0) = 1 \tag{7}$$

The form of (4a) is intended to indicate that the problem is simply solvable for the case of current profiles without curvature, or $\sigma_{,zz} = 0$. The model (4a)-(4c) has been used in a number of studies of arbitrary or idealized velocity distributions; see reviews by Peregrine (1976), Jonsson (1990) and Thomas & Klopman (1997). For the general case of arbitrary $\mathbf{U}(z)$, Voronovich (1976) derived a conservation law, in the geometric optics approximation, for an adiabatic invariant corresponding to the wave action density, with $\mathcal{N}$ and $\boldsymbol{\mathcal{F}}$ in (1) given by

$$\mathcal{N} = -\frac{\rho}{4}\int_{-h}^{0}\frac{1}{\sigma^2k^2}\sigma_{,zz}|w|^2dz + \rho\left[\left(\frac{g}{2\sigma^3}+\frac{1}{4\sigma^2k^2}\sigma_{,z}\right)|w|^2\right]_{z=0} \tag{8a}$$

$$\begin{aligned}\boldsymbol{\mathcal{F}} &= \frac{\rho}{4}\int_{-h}^{0}\left(-\frac{\mathbf{U}}{\sigma^2k^2}\sigma_{,zz}+\frac{1}{\sigma k^2}\mathbf{U}_{,zz}-\frac{2\mathbf{k}}{k^2}\right)|w|^2dz \\ &+\left\{\rho\left[\mathbf{U}(\frac{g}{2\sigma^3}+\frac{1}{4\sigma^2k^2}\sigma_{,z})-\frac{1}{4\sigma k^2}\mathbf{U}_{,z}+\frac{g\mathbf{k}}{2\sigma^2k^2}\right]|w|^2|\right\}_{z=0}.\end{aligned} \tag{8b}$$

These results may be written in more compact form using the substitution

(7), giving

$$\mathcal{N} = \frac{E_0}{\sigma_s}\left[1+\frac{\sigma_s}{2gk^2}\left(\sigma_{,z}(0)-\sigma_s^2\int_{-h}^{0}\sigma^{-2}\sigma_{,zz}f^2dz\right)\right] \tag{9a}$$

$$\begin{aligned}\boldsymbol{\mathcal{F}} &= \frac{E_0}{\sigma_s}\left[\mathbf{U}_s+\mathbf{c}_{rs}\left(1-\frac{\sigma_s^2}{g}\int_{-h}^{0}f^2dz\right)\right.\\ &\left.+\frac{\sigma_s}{2gk^2}\left(-\mathbf{A}(0)+\sigma_s^2\int_{-h}^{0}\sigma^{-2}\mathbf{A}_{,z}f^2dz\right)\right]\end{aligned} \tag{9b}$$

where $E_0 = (1/2)\rho g a^2$ is the energy density for a wave on a depth-uniform current, $\mathbf{c}_{rs} = (\sigma_s/k)\hat{\mathbf{k}}$ is the wave phase velocity relative to the surface current, and

$$\mathbf{A}(z) = \sigma(z)\mathbf{U}'(z) - \sigma'(z)\mathbf{U}(z) \tag{10}$$

The adiabatic invariant $\mathcal{N}$ in (8a) or (9a) is not clearly in the form of wave energy divided by frequency, as expected from the work of Bretherton & Garrett (1968), but takes on this form in cases where analytic results for $\tilde{w}$ are available, such as the special case of waves on a current with constant vertical shear (Jonsson *et al.*, 1978). Additionally, the flux vector $\boldsymbol{\mathcal{F}}$ in (8b) or (9b) isn't clearly in the form of action density times group velocity, $\mathcal{N}\mathbf{c}_{ga}$, but can also be shown to be in this form for the constant shear case.

Analytic solutions for progressive waves for the problem (4a)-(4c) are limited to the cases of currents with constant vertical shear, including the uniform-over-depth limit of zero shear. For more complex profiles, results may be obtained using perturbation solutions due to Stewart & Joy (1974) for deep water or Skop (1987) for finite depth, with solutions extended to second order by KC89. Shrira (1993) has further demonstrated how series solutions for deep water may be extended to high order. Ellingsen & Li

(2017) have extended the basis for perturbation solutions to include currents with constant shear in the leading order solution. Alternately, numerical solutions may be obtained using a variety of methods, including shooting methods (Fenton, 1973; Dong & Kirby, 2012) or an iterative approach to the boundary value problem described by Li & Ellingsen (2019), used below in Section 5.

3. Approximate solution and analysis of action and action flux expressions

KC89 considered the propagation of a wave train which was colinear with the mean current, and assumed that $F = U/c \ll 1$, where F represents a Froude number for the mean flow, U describes the current magnitude, and c is a reference phase speed, usually taken to be $\sqrt{gh}$. Here, we consider the case of arbitrary orientation of wave and current, and allow for strong currents $F = O(1)$, in which case the current enters the wave dispersion relation at leading order. This generalization of the results of Skop (1987) and KC89 has also been described previously by Dong & Kirby (2012) and Ellingsen & Li (2017). The results are repeated here as a basis for discussion of the approximate forms for action density and flux. We also modify the treatment of the surface boundary condition for $f(z)$ from prior studies in order to simplify numerical applications.

3.1. Scaling framework and series solution

An appropriate scaling of the problem and the resulting perturbation solution is described in Appendix A, and leads to a problem characterized by parameters F (describing the strength of the current), ϵ (characterizing the magnitude of current shear), and μ (characterizing the ratio of water depth to wavelength). Here, we consider the case of $\mu, F = O(1)$ and $\epsilon \ll 1$, which allows for the development of a formally ordered expansion in powers of ϵ. The solution to the resulting problem is carried out to $O(\epsilon)$ in Appendix A. In particular, the intrinsic frequency σ is approximated by

$$\sigma(z) = \omega - \mathbf{k} \cdot \mathbf{U}(z) = (\omega - \mathbf{k} \cdot \tilde{\mathbf{U}}) - \epsilon \mathbf{k} \cdot \mathbf{U}_1(z) = \tilde{\sigma} + \epsilon \sigma_1(z) \tag{11}$$

where

$$\tilde{\mathbf{U}} = \frac{2k}{\sinh 2kh} \int_{-h}^{0} \mathbf{U}(z) \cosh 2k(h+z) dz \tag{12}$$

and $\mathbf{U}_1(z) = \mathbf{U}(z) - \tilde{\mathbf{U}}$. The vertical velocity w is given to $O(1)$ by

$$w(z) = -i\tilde{\sigma} a f_0(z) \tag{13}$$

with

$$f_0(z) = \frac{\sinh k(h+z)}{\sinh kh} \tag{14}$$

and the dispersion relation

$$\tilde{\sigma}^2 = gk \tanh kh \tag{15}$$

The leading-order correction to the vertical shape function f is given by

$$f_1(z) = \frac{1}{2\tilde{\sigma}} \left[I_1(0) - I_1(z) - (I_2(0)/\tanh kh) \right] f_0(z) + \frac{I_2(z)}{2k\tilde{\sigma}} f_{0,z}(z) \tag{16}$$

where, in contrast to KC89 or Quinn *et al.* (2017), we retain the homogeneous part of the solution for $f_1(z)$ in order to specify a boundary condition $f_1(0) = 0$, as discussed in Appendix A. The integrals in (16) are given by

$$\begin{aligned} I_1(z) &= \sinh^{-1} kh \int_{-h}^{z} \hat{\mathbf{k}} \cdot \mathbf{U}_{,\xi\xi}(\xi) \sinh 2k(h+\xi)\, d\xi \\ I_2(z) &= \sinh^{-1} kh \int_{-h}^{z} \hat{\mathbf{k}} \cdot \mathbf{U}_{,\xi\xi}(\xi)(\cosh 2k(h+\xi) - 1)\, d\xi \end{aligned} \tag{17}$$

The solution for w up to $O(\epsilon)$ is then given by

$$\tilde{w} = -i\sigma_s a[f_0(z) + f_1(z)] \tag{18}$$

with $\sigma_s = \tilde{\sigma} + \sigma_1(0) = \tilde{\sigma} - \mathbf{k} \cdot \mathbf{U}_1(0) = \tilde{\sigma} - \mathbf{k} \cdot (\mathbf{U}_s - \tilde{\mathbf{U}})$. For later use, the depth dependent intrinsic frequency $\sigma(z)$ can also be written as

$$\sigma(z) = \sigma_s - \mathbf{k} \cdot (\mathbf{U}(z) - \mathbf{U}_s) \tag{19}$$

3.2. Approximate expressions for action density and flux

Results presented here favor a framework where quantities are defined primarily in a frame moving with the velocity $\tilde{\mathbf{U}}$, with associated intrinsic frequency $\tilde{\sigma}$. This choice is not unique, and is often replaced by representations based on conditions at the water surface. A particular example is that of Quinn *et al.* (2017), who developed asymptotic expressions for $\mathcal{N}$ and $\boldsymbol{\mathcal{F}}$ by starting from (8a) and (8b) and introducing expansions for w, σ (or phase speed C), and for the amplitude of their w relative to surface wave amplitude a.

Here, we pursue a different approach starting from (9a) and (9b), where the original expressions have been simplified using the transformation (7) and the known properties of the problem prior to expansion. This transformation and the simplified expressions (9a) and (9b) are still an exact description of the original problem. In order to assess the difference between the two choices of reference frames, we develop a generic approximation which specifies neither, and then specialize it to the two frames of interest. The basic development of the framework is described in Appendix B, and leads to (B.4) and (B.18) for action density $\mathcal{N}_0$ and flux $\boldsymbol{\mathcal{F}}_0$ in which a final choice of reference frame velocity and leading order dispersion relation has not been made. As in Quinn *et al.* (2017), the choice of surface conditions as a reference leads to an expression for action density containing an $O(\epsilon)$ component, where ϵ here is basically similar to ϵ_5 in Quinn *et al.* The expression is given here by (B.19) or

$$\mathcal{N}^* = \frac{E_0}{\sigma_s}\left[1 + \epsilon\frac{(\sigma_s - \tilde{\sigma})}{\sigma_s}\right] \tag{20}$$

This expression is similar in form to (4.2) in Quinn *et al.* (2017), but the $O(\epsilon)$ components in the two studies do not appear to have a close correspondence. This is discussed further in section 7.1. In contrast, the approximation resulting from the choice of the depth-weighted current reference frame gives the estimate (B.20) or

$$\tilde{\mathcal{N}} = \frac{E_0}{\tilde{\sigma}} + O(\epsilon^2) \tag{21}$$

This result was suggested by KC89 based on an analysis of the constant shear case of Section 4, but was not formally established there as a general result. We note that the two formulas (20) and (21) are asymptotically equivalent to within the accuracy of the approximation, which can easily be established by substituting between σ_s and $\tilde{\sigma}$. However, actual numerical values from the two expressions are seen to diverge in particular examples, as will be shown for a linear shear profile in section 4 and for a wind driven current in section 7.1.

It is clear, from these results, that a formulation in terms of $\tilde{\sigma}$ and $\tilde{\mathbf{U}}$ is a more compact version of the approximation. Similar treatment for the action flux (B.18) leads to the expressions

$$\boldsymbol{\mathcal{F}}^* = \frac{E_0}{\sigma_s}\left[\hat{\mathbf{U}} + \mathbf{c}_{grs} + \epsilon\left(\frac{\mathbf{U}_s}{\sigma_s} + \frac{\hat{\mathbf{k}}}{k}(1-G)\right)(\sigma_s - \tilde{\sigma})\right] + O(\epsilon^2) \qquad (22)$$

and

$$\tilde{\boldsymbol{\mathcal{F}}} = \frac{E_0}{\tilde{\sigma}}\left[\hat{\mathbf{U}} + \tilde{\mathbf{c}}_{gr}\right] + O(\epsilon^2) \qquad (23)$$

We note the striking result that both versions of the approximate action flux identify $\hat{\mathbf{U}} = \tilde{\mathbf{U}} + \hat{\mathbf{k}}(\mathbf{k}\cdot\tilde{\mathbf{U}}_{,k})$ as the correct current advection velocity. The appearance of $\hat{\mathbf{U}}$ results from the treatment of the integral of the product of the zeroth and first order shape functions f_0 and f_1; see (B.13) - (B.17). The current $\hat{\mathbf{U}}$ is the vector form of the advection velocity suggested by KC89 and discussed recently by BKD17. This result may be obtained directly from the definition of group velocity,

$$\begin{aligned}
\mathbf{c}_{ga} &= \omega_{,\mathbf{k}} = (\sigma + \mathbf{k}\cdot\tilde{\mathbf{U}})_{,\mathbf{k}} \\
&= \hat{\mathbf{k}}\sigma_{,k} + \tilde{\mathbf{U}} + \hat{\mathbf{k}}\left(\mathbf{k}\cdot\tilde{\mathbf{U}}_{,k}\right) \\
&= \mathbf{c}_{gr} + \hat{\mathbf{U}} \qquad (24)
\end{aligned}$$

Unlike the expressions (20) and (21) for $\mathcal{N}$, the expressions for $\boldsymbol{\mathcal{F}}$ do not appear to be consistent with each other to the order of approximation considered. An attempt to rearrange (22) to the form of (23) to within cancellation of $O(\epsilon^2)$ terms leads to the result

$$\boldsymbol{\mathcal{F}}^* = \frac{E_0}{\tilde{\sigma}}\left[\hat{\mathbf{U}} + \tilde{\mathbf{c}}_{gr} + \epsilon\frac{\hat{\mathbf{k}}}{k}(1-G)(\sigma_s - \tilde{\sigma})\right] \qquad (25)$$

where the remaining term at $O(\epsilon)$ results from the treatment of the I_4 integral in (B.11) (or the first occurrence of $(1-G)$ in (B.18)), where no $O(\epsilon)$ expansion term occurs in the surface-oriented expression, whereas the $O(\epsilon)$ expansion term occurring in the $\tilde{\mathbf{U}}$-oriented expression cancels the second $(1-G)$ term contributed by the integral I_5 in (B.17). A similar attempt to work from (23) to (22) also leaves an $O(\epsilon)$ residual which differs from the one in (22).

The results (20) and (22) for $\mathcal{N}^*$ and $\boldsymbol{\mathcal{F}}^*$ are expected to be far accurate representations of action density and flux than simple constructs based on surface or depth-averaged currents, but the relative accuracy of the two asymptotic approaches remains to be examined. We will take up this question again in sections 4 and 7.1.

4. Waves on currents with constant shear

In this section, we examine the accuracy of the asymptotic expressions for $\mathcal{N}$ and $\boldsymbol{\mathcal{F}}$ for the case of waves on a current with constant vertical shear. This case has been studied extensively, with the basic solution described for collinear propagation in one horizontal dimension (Thompson, 1949) and subsequently extended to two horizontal dimensions for waves oblique to the current (Craik, 1968; Ellingsen, 2016, among others). Ellingsen (2016) provides a clear description of the influence of wave orbital motion on the vorticity field for the case of oblique waves. Jonsson *et al.* (1978) gave expressions for the action density and flux for the 1D case of co-linear wave and current; the extension to the general case is given below based on the theory of Voronovich (1976). In this section, we determine the accuracy of the approximate expressions in a space covering variations of kh, F, θ (representing the angle between the wave direction and the surface current), and a shear parameter α defined below. Consider a current profile with constant shear (and possible rotation) given by

$$\mathbf{U}(z) = \mathbf{U}_s + \mathbf{\Omega} z \tag{26}$$

The current shear $\mathbf{\Omega}$ does not have to be collinear with either $\mathbf{U}_s$ or $\mathbf{k}$ (Figure 1). In this case, the BVP (4a-4c) simplifies and is given by

$$\begin{aligned} \sigma(w_{,zz} - k^2 w) &= 0; \qquad -h \le z \le 0 \\ \sigma_s^2 w_{,z}(0) - (gk^2 - \sigma_s \mathbf{k}\cdot\mathbf{\Omega}) w(0) &= 0 \\ w(-h) &= 0 \end{aligned} \tag{27}$$

The possibility of $\sigma(z)$ taking on a value of zero at a critical level is not typically of interest in surface wave dynamics; see also Ellingsen & Li (2017). The solution to (27) is given by

$$
\begin{aligned}
w(z) &= -i\sigma_s a f(z) && (28)\\
\mathbf{u}(z) &= \sigma_s a \left(\frac{1}{\sigma} (\hat{\mathbf{k}}(\hat{\mathbf{k}} \cdot \boldsymbol{\Omega}) - \boldsymbol{\Omega}) f(z) + \frac{\hat{\mathbf{k}}}{k} f_{,z}(z) \right) && (29)\\
p(z) &= \frac{\rho \sigma_s a}{k} \left((\hat{\mathbf{k}} \cdot \boldsymbol{\Omega}) f(z) + \frac{\sigma}{k} f_{,z}(z) \right) && (30)
\end{aligned}
$$

with vertical shape function

$$
f(z) = \frac{\sinh k(h+z)}{\sinh kh} \tag{31}
$$

and with dispersion relation

$$
\sigma_s^2 = (gk - \sigma_s \hat{\mathbf{k}} \cdot \boldsymbol{\Omega}) \tanh kh \tag{32}
$$

Constant current shear affects the vertical structure of wave orbital velocity and wave pressure by modifying the dispersion relation and twisting wave horizontal velocity in the current shear direction. Absolute and relative phase speed vectors are related by

$$
\mathbf{c}_a = \mathbf{c}_{rs} + \hat{\mathbf{k}}(\hat{\mathbf{k}} \cdot \mathbf{U}_s) \tag{33}
$$

where $\mathbf{c}_a = c_a \hat{\mathbf{k}} = (\omega/k)\hat{\mathbf{k}}$ and $\mathbf{c}_{rs} = c_{rs}\hat{\mathbf{k}} = (\sigma_s/k)\hat{\mathbf{k}}$, with subscripts s denoting values at the SWL $z = 0$. From (32), an expression for c_{rs} is given by

$$c_{rs} = \frac{1}{2k}\left[\pm(4gk\tanh kh + (\hat{\mathbf{k}}\cdot\mathbf{\Omega}\tanh kh)^2)^{1/2} - \hat{\mathbf{k}}\cdot\mathbf{\Omega}\tanh kh\right] \tag{34}$$

Inserting the wave solutions in (9a) and (9b) gives exact expressions for the action density and flux, given by

$$\mathcal{N} = \frac{E_0}{\sigma_s}\left(1 - \frac{\hat{\mathbf{k}}\cdot\mathbf{\Omega}c_{rs}}{2g}\right) \tag{35}$$

and

$$\boldsymbol{\mathcal{F}} = \mathcal{N}\mathbf{c}_{ga}; \qquad \mathbf{c}_{ga} = \mathbf{U}_s + \mathbf{c}_{grs} \tag{36}$$

The relative group velocity $\mathbf{c}_{grs}$ is given by

$$\mathbf{c}_{grs} = \sigma_{s,\mathbf{k}} = \frac{\hat{\mathbf{k}}[g(1+G)c_{rs}] + [\hat{\mathbf{k}}(\hat{\mathbf{k}}\cdot\mathbf{\Omega})(1-G) - \mathbf{\Omega}]c_{rs}^2}{2g - (\hat{\mathbf{k}}\cdot\mathbf{\Omega})c_{rs}} \tag{37}$$

Turning to the perturbation solution of Section 3, we obtain results to $O(\epsilon)$ in the $\tilde{\mathbf{U}}$ reference frame and compare them to the full solution to determine their range of validity. The weighted current $\tilde{\mathbf{U}}$ is given by

$$\tilde{\mathbf{U}} = \mathbf{U}_s - \mathbf{\Omega}\frac{\tanh kh}{2k} \tag{38}$$

and the corresponding flux advection velocity $\hat{\mathbf{U}}$ is then given by

$$\hat{\mathbf{U}} = \tilde{\mathbf{U}} + \hat{\mathbf{k}}(\mathbf{k}\cdot\tilde{\mathbf{U}}_{,k}) = \mathbf{U}_s - \frac{\tanh kh}{2k}\Big(\mathbf{\Omega} - \hat{\mathbf{k}}(\hat{\mathbf{k}}\cdot\mathbf{\Omega})(1-G)\Big) \tag{39}$$

with action $\tilde{\mathcal{N}}$ and action flux $\tilde{\boldsymbol{\mathcal{F}}}$ determined by (21) and (23).

The % error $100(1 - \tilde{\mathcal{N}}/\mathcal{N})$ for the first order perturbation approximation of the action density (21) compared to the exact result from (35) is shown in Figure 2 for $0.1 < kh < 10$, $-\pi/2 < \theta < \pi/2$, relative angle $\beta = 0$ and for different choices of current strength and shear. Additional results for $\beta = \pi/4$ and $\pi/2$ are provided as Figures C1 and C2 in the Supplement, Appendix C. (Angles θ and β represent the orientation of $\mathbf{k}$ and $\mathbf{\Omega}$ relative to the surface current U_s, as indicated in Figure 1. Current strength is represented through a Froude number based on surface current speed, $F = |\mathbf{U}_s|/\sqrt{gh}$, while shear is represented by dimensionless parameter $\alpha = h|\mathbf{\Omega}|/|\mathbf{U}_s|$.

The results show a considerably improved accuracy in the predicted action density, compared to values constructed using other common approaches, such as using the surface velocity $\mathbf{U}_s$, with $\mathcal{N}$ given by $\mathcal{N}_s = E_0/\sigma_s$; Figures C3 - C5 in Supplement) or depth-averaged velocity $\overline{\mathbf{U}}$, with $\mathcal{N}$ given by $\overline{\mathcal{N}} = E_0/\overline{\sigma}$, $\overline{\sigma} = \omega - \mathbf{k} \cdot \overline{\mathbf{U}}$; Figures C6 - C8 in Supplement). Opposing currents require a more complex calculation of blocking conditions; this limit is not crucial to the development here and deserves it's own treatment in connection with wave propagation near buoyant plumes and other frontal features; see BKD17 for examples of the relative magnitudes of errors in those cases.

An extensive comparison of the correct and approximate action flux velocities for the 1D case has been discussed in BKD17. Figure 3 shows the composite error of $|\tilde{\boldsymbol{\mathcal{F}}}|$ as a function of kh and θ for $\beta = 0$ using the first order perturbation approximation, with additional results for $\beta = \pi/4$ and $\pi/2$ in Figures C9 and C10 in the Supplement. Results for the same range of parameters using the surface and depth-average current values are shown in Figures C11 - C16 in the Supplement.

As mentioned is section 3.2, the relative accuracy of the two asymptotic approaches in the frame of reference based on the surface current and the depth weighted current remains to be examined. Figure 4 and 5 provide a simple comparison of equations (20) vs (21), and (22) vs (23). The comparison is done for a linear shear profile with variation of α, F and kh, with $\theta = 0$ and $\beta = 0$. The gain in accuracy provided by the estimates $\tilde{\mathcal{N}}$ and $\tilde{\boldsymbol{\mathcal{F}}}$ is shown, in spite of the two expressions being asymptotically equivalent within the accuracy of the approximation.

5. Columbia River velocity profile

In this section, we compare the action densities obtained from different approximations using a measured current profile from the Mouth of the Columbia River (MCR), where fresh riverine water meets salty seawater and the current becomes strongly sheared due to stratification and tidal effects. Here, we select a sample velocity profile collected by a pole-mounted ADCP during the RISE project (Kilcher & Nash, 2010). The profile, shown in Figure 6, was also used in BKD17, and represents a maximum ebb condition for the time frame covered by the file. The water depth is $h = 25\,m$, the normalized shear parameter for this current profile is $\alpha \sim 8$, which indicates a strongly sheared current, while the Froude number is $F \sim 0.15$. The current profile is assumed to be unidirectional.

We consider the case of waves propagating landward against the opposing current. We follow a general procedure of fitting polynomials to either measured profiles or profiles taken from gridded model results in order to establish a basis for computing weighted current values. Expressions below are based on the form

$$\mathbf{U}(z) = |\mathbf{U}_s| \sum_{n=0}^{N} \mathbf{a}_n (\frac{z}{h})^n \tag{40}$$

with current speed referenced to the surface value U_s and with dimensionless a_n's. (Note that $a_0 = 1$ due to the normalization by the surface current velocity, while $a_1 = \Omega_s h/U_s \sim \alpha$, where Ω_s is the current shear at the surface.) Calculations here are carried out using $N = 6$, with the fitted profile for the demonstration case also shown in Figure 6. For the given profile the coefficients in (40) are then given by

$$\begin{aligned} U(z) &= -2.28 \Big(1 + 8.22\frac{z}{h} + 40.26(\frac{z}{h})^2 + 120.52(\frac{z}{h})^3 \\ &\quad +197.04(\frac{z}{h})^4 + 160.36(\frac{z}{h})^5 + 50.85(\frac{z}{h})^6 \Big) \end{aligned} \tag{41}$$

In the absence of an analytic solution, a numerical method is used to solve the Rayleigh equation. In BKD17 the procedure used by Dong & Kirby (2012) was considered to solve the boundary value problem. The vertical velocity $w(z)$ was found by solving a Riccati equation using a shooting method due to Fenton (1973), also discussed in KC89. Here, we use the Direct Integration Method (DIM) presented by Li & Ellingsen (2019) which is faster and easier to parallelize than the shooting method. The method starts by rewriting (4a) - (4c) with the substitution (7) as

$$(f_{,zz} - k^2 f) = \frac{\sigma_{,zz}(z)}{\mathbf{k}\cdot\Delta\mathbf{U} - kc_{rs}} f; \qquad -h \leq z \leq 0 \tag{42a}$$

$$c_{rs}^2 - c_{rs} I_c(c_{rs}) - {c_0}^2 = 0 \tag{42b}$$

where c_{rs} is the relative wave phase speed at the surface and

$$I_c(c_{rs}) = \frac{\mathbf{k}\cdot\mathbf{U}_{,z}(0)\tanh kh}{k^2} + c_{rs}\int_{-h}^{0} \frac{\mathbf{k}\cdot\mathbf{U}_{,z}(z) f(z)\sinh k(z+h)}{k(\mathbf{k}\cdot\Delta\mathbf{U} - kc_{rs})\cosh kh}\, dz \tag{43a}$$

$${c_0}^2 = \frac{g}{k}\tanh kh \tag{43b}$$

$$f(z) = w(z)/w(0) \tag{43c}$$

$$\Delta\mathbf{U} = \mathbf{U}(z) - \mathbf{U}_s \tag{43d}$$

The DIM method treats equations (42a) and (42b) as two coupled equations with f and c_{rs} as the unknowns, and then obtains the numerical solution to the set of equations. The results are used in (8a) and (8b) to obtain numerical values for wave action density and flux, which are taken to be the reference "exact" solutions.

The accuracy of the first order perturbation approximation of the wave action density $\tilde{\mathcal{N}}$ and wave action flux $\tilde{\boldsymbol{\mathcal{F}}}$ relative to the numerical solution obtained from the DIM is shown in Figure 7. The results are plotted against a parameter kz_0 instead of kh where z_0 is specifically defined assuming a linear profile down from the surface until the current falls to zero at depth z_0. In this case the z_0 would be $z_0 = U_s/U_s'(0) \sim 3m$.

Similar to the linear shear case, the results show improved accuracy in the estimate of action density compared to the common approaches using depth averaged or surface current values, displayed as Figures C17 - C20 in the Supplement.

6. Taylor series expansion of $\tilde{\mathcal{N}}(\mathbf{k})$ and $\tilde{\mathcal{F}}(\mathbf{k})$ about $\mathbf{k}^p$.

The use of the first order correction to the group velocity $\hat{U}$ and the more simplified procedure of using a single value $\hat{U}(k^p)$ instead of the frequency dependent form has been investigated in BKD17 for the case of co-linear waves and current. BKD17 suggested an alternate strategy, involving a Taylor series expansion about the peak frequency, which should significantly extend the range of accuracy of current information available to the wave model with minimal additional data transfer between wave and circulation models. Writing the components of the effective advection velocity as $\hat{\mathbf{U}} = (\hat{U}_i, \hat{U}_j)$, the Taylor expansion in component form is given by

$$\hat{U}_{Ti}(\mathbf{k}) = \hat{U}_i(\mathbf{k}^p) + (\mathbf{k} - \mathbf{k}^p) \cdot \frac{\partial \hat{U}_i}{\partial \mathbf{k}}\Big|_{k^p} + O(|\mathbf{k} - \mathbf{k}^p|^2) \qquad (44)$$

where subscript T denotes the value obtained from the truncated series. Using the relation between $\hat{\mathbf{U}}$ and $\tilde{\mathbf{U}}$ gives

$$\begin{aligned} \frac{\partial \hat{U}_i}{\partial \mathbf{k}} &= \frac{\partial \tilde{U}_i}{\partial \mathbf{k}} + \frac{\partial}{\partial \mathbf{k}}(\frac{k_i}{k}\mathbf{k}\cdot \frac{\partial \tilde{\mathbf{U}}}{\partial k}) \\ &= \hat{\mathbf{k}}\frac{\partial \tilde{U}_i}{\partial k} + \frac{k_i}{k}\left(\frac{\partial \tilde{\mathbf{U}}}{\partial k}\right) + \hat{\mathbf{k}}\left[\frac{k_i}{k}(\mathbf{k} \cdot \frac{\partial^2 \tilde{\mathbf{U}}}{\partial k^2})\right] \end{aligned} \qquad (45)$$

The Taylor series expansion in component form is then given by

$$\begin{aligned}\hat{U}_{Ti}(\mathbf{k}) &= \tilde{U}_i(\mathbf{k}^p) + \frac{k_i^p}{k}(\mathbf{k}\cdot\frac{\partial\tilde{\mathbf{U}}}{\partial k})\Big|_{\mathbf{k}^p} + \frac{\mathbf{k}^p}{k}\cdot(\mathbf{k}-\mathbf{k}^p)\frac{\partial\tilde{U}_i}{\partial k}\big|_{k^p} \\ &+ \frac{k_i^p}{k}(\mathbf{k}-\mathbf{k}^p)\cdot\frac{\partial\tilde{\mathbf{U}}}{\partial k}\Big|_{k^p} \\ &+ \frac{k_i^p}{k}\frac{\mathbf{k}^p}{k}\cdot(\mathbf{k}-\mathbf{k}^p)\big(\mathbf{k}^p\cdot\frac{\partial^2\tilde{\mathbf{U}}}{\partial k^2}\Big|_{k^p}\big) \end{aligned} \qquad (46)$$

The same approach is used to calculate the intrinsic frequency relative to the value at the peak wave number as

$$\tilde{\sigma}_T(\mathbf{k}) = \omega - \mathbf{k}\cdot\tilde{\mathbf{U}}\Big|_{k_p} - \frac{\mathbf{k}^p}{k}\cdot(\mathbf{k}-\mathbf{k}^p)(\mathbf{k}\cdot\tilde{\mathbf{U}}_{,k}\Big|_{k_p}) \qquad (47)$$

where we take advantage of the fact that the local value of ω is known for each frequency component.

Returning to the case of a current with constant shear, we show results for the accuracy of the action density $\tilde{\mathcal{N}}_T$ for three peak wave numbers corresponding to $k^p h = 1, 2$ and 3 in Figures 8-10, with the peak direction $\theta^p = 0$, the current non-rotational over depth ($\beta = 0$) and a range of directions of $\pm\pi/3$. Figures C21 - C23 in the Supplement compare the action flux approximation $\tilde{\boldsymbol{\mathcal{F}}}_p$ for the same cases. Corresponding results for action density $\tilde{\mathcal{N}}$ for the MCR current profile are provided in Figure 11 for $k_p h = 1, 2$ and the directional spreading of $\pi/5$, while the comparison for the action flux $\tilde{\boldsymbol{\mathcal{F}}}_T$ is shown in Figures C24 and C25 in the Supplement.

Overall, it is seen that the Taylor series approach provides a robust estimate for action density and action flux, using only information about the depth-weighted current velocity at the spectral peak frequency. These expressions should be relatively simple to implement in spectral wave models, but implementation would require the calculation of $\tilde{\mathbf{U}}(\mathbf{k}_p)$, $\tilde{\mathbf{U}}_{,k}(\mathbf{k}_p)$ and $\tilde{\mathbf{U}}_{,kk}(\mathbf{k}_p)$ in the circulation model using the 3D velocity field available there, and the passage of the three vector quantities at each grid point, rather than the passage of as single current velocity vector as presently implemented.

7. Discussion and Conclusions

7.1. Comparison to results of Quinn et al. *(2017)*

Despite the similarity in approach to developing approximations for action density and flux in this study and that of Quinn *et al.* (2017), the results are significantly different, as revealed in a comparison of the two results for the analytic case of a current with constant shear. For this case, $\mathbf{U}'' = 0$ simplifies the result for action density (4.2) in Quinn *et al.*. Their general result for action density is given by

$$\mathcal{N}^{Q17} = \frac{E_0}{\sigma_s}(1 + \epsilon_5 \mathcal{R}_1); \qquad \mathcal{R}_1 = -2\mathcal{I}_2 \sinh kh - \frac{1}{c_0}\left(\frac{2}{\sinh 2kh}\mathcal{I}_3 + c_1\right) \quad (48)$$

we see that $\mathcal{I}_2 = 0$ from (4.4). Both terms $2\mathcal{I}_3(0)/\sinh 2kh$, evaluated directly and c_1 in the bracketed expression in $\mathcal{R}_1$ are equivalent to an expression $\hat{\mathbf{k}} \cdot \tilde{\mathbf{U}}$ as used here

For $z = 0$, it is also apparent that the first term in parentheses is the projection of the weighted average velocity, $\hat{\mathbf{k}} \cdot \tilde{\mathbf{U}}$, which follows directly from the definition (12) here and the expression for $\mathcal{I}_3$ as given in Quinn *et al.*'s (4.4). The evaluation of c_1 from (C.7) is more ambiguous. If $\mathcal{I}_1$ is interpreted as usual as the starting point for the definition of $\tilde{\mathbf{U}}$ after two integrations, then c_1 also is equal to $\hat{\mathbf{k}} \cdot \tilde{\mathbf{U}}$. This would then give an expression for $\mathcal{N}$ in our notation as

$$\mathcal{N}^{Q17} = \frac{E_0}{\sigma_s}\left[1 - \frac{2\mathbf{k} \cdot \tilde{\mathbf{U}}}{\tilde{\sigma}} + O(\epsilon^2)\right] \tag{49}$$

On the other hand, if the expression is taken literally for the constant shear case under development, then c_1 evaluates to $c_1 = \hat{\mathbf{k}} \cdot (\mathbf{U}_s - (c_0^2/2g)\mathbf{U}_{,z}(0))$, which referring to (38), is again the depth-weighted current for this special case, giving the expression (49) again. It is clear that this expression cannot be correct, as $\mathcal{N}^{Q17}$ would have to reduce to E_0/σ_s in the limit of a depth-uniform current, where $\tilde{\mathbf{U}} = \mathbf{U}_s$. We are thus not able to explain the discrepancies between our results written in terms of surface values, and the expressions provided by Quinn *et al.* (2017).

In contrast, the result obtained in the present study can be written as

$$\tilde{\mathcal{N}} = \frac{E_0}{\sigma_s}\left[1 - \frac{\mathbf{k}}{\tilde{\sigma}} \cdot (\mathbf{U}_s - \tilde{\mathbf{U}}) + O(\epsilon^2)\right] \tag{50}$$

Quinn *et al.* go on to suggest (below their (4.4)) that using the surface current in the estimate of action instead of depth-averaged current would be a reasonable no-cost extension in existing models. This suggestion corresponds to the results for $\mathcal{N}_s$ and $\boldsymbol{\mathcal{F}}_s$ shown in the Supplement, Appendix C. From the results there, it is clear that the increase in accuracy afforded by using surface current instead of depth average current is apparent only for relatively short waves, whereas the proper use of the perturbation solution, or expansions based on that solution, is advantageous at all water depths.

In order to examine the relative predictions of the asymptotic forms (20) + (22) vs. (21) + (23), and to establish a basis for comparing our error estimates to a case examined by Quinn *et al.* (2017), we have repeated their analysis of a current profile given by Wu & Tsanis (1995) and presented in their Section 5 and Figures 1-4. The current profile is given by

$$U(z) = Au_* \ln(1 + \frac{z}{z_s}) + Bu_* \ln(1 - \frac{z}{z_b + h}) \tag{51}$$

in which

$$\begin{aligned} A &= \frac{q_2}{p_1 q_2 - q_1 p_2}; \qquad B = -\frac{q_1}{p_1 q_2 - q_1 p_2} \\ q_1 &= (1 + z_s/h)\ln(1 + h/z_s) - 1; \quad q_2 = z_s/h \ln(1 + h/z_b) - 1 \\ p_1 &= \gamma z_s/h; \qquad p_2 = \gamma z_s/z_b \end{aligned} \tag{52}$$

where z_b and z_s are characteristic viscous sublayer thicknesses at the bottom and surface respectively, and γ is a constant to characterize the intensity of the turbulence. The origin of the z-coordinate is located at the bottom for this velocity profile and the direction is upward. A lengthscale δ_s is taken to be the depth at which the current velocity falls to zero, and is used as the basis for a relative wavelength parameter $k\delta_s$ used in plots presented below and by Quinn *et al.*.

Figure 12 shows errors for action density $\tilde{\mathcal{N}}$ and flux $\tilde{\boldsymbol{\mathcal{F}}}$ using the asymptotic expressions (21) and (23) with variation of $k\delta_s$ and Froude number U_s/c_0. The axis has been modified to be in the same format as Quinn *et al.* (2017) figure 2 for comparison, however our Froude number is for a larger range $0 < U_s/c_0 < 1$, while they have only provided results for $0 < U_s/c_0 < 0.3$. Profile parameters are given by $z_s = 2.2 \times 10^{-}4\,h$,

$z_b = 1.4 \times 10^{-4}h$, $\gamma = 0.35$ and $h = 100\,m$. The thickness of the upper layer is $\delta_s = 0.34\,h$ in this case. Comparison between the results and the plots presented in their figure 2(a) and 2(d) demonstrate the accuracy gain in our approximation. Corresponding plots for our estimates $\mathcal{N}^*$ and $\mathbf{c}^*_{ga} = \boldsymbol{\mathcal{F}}^* / \mathcal{N}^*$ based on (20) and (22) are provided in Figure 13, and show a marked decrease in accuracy compared to the values $\tilde{\mathcal{N}}$ and $\tilde{\mathbf{c}}_{ga} = \tilde{\boldsymbol{\mathcal{F}}} / \tilde{\mathcal{N}}$ in spite of the demonstrated asymptotic equivalence of $\tilde{\mathcal{N}}$ and $\mathcal{N}^*$, with errors based on $\tilde{\mathcal{N}}$ and $\tilde{\boldsymbol{\mathcal{F}}}$ being up to 100 times smaller. We also note that our estimates for $\mathcal{N}^*$ and $\boldsymbol{\mathcal{F}}^*$ in the frame of reference based on the surface current is by far more accurate than the results shown in Quinn *et al.* (2017).

7.2. Conclusions

The results here clearly show that leading order asymptotic expressions for action density and flux are both more compact and more accurate numerically when written in terms of a depth-weighted current $\tilde{\mathbf{U}}$ and corresponding intrinsic frequency $\tilde{\sigma}$. The asymptotic expressions written in the form of (21) and (23), repeated here as

$$\tilde{\mathcal{N}} = \frac{E_0}{\tilde{\sigma}} + O(\epsilon^2); \quad \tilde{\boldsymbol{\mathcal{F}}}(\hat{\mathbf{U}} + \tilde{c}_{gr}) + O(\epsilon^2) \tag{53}$$

defer the appearance of terms which are not in the standard form for action and flux to second order in the small parameter ϵ characterizing the weak shear in the depth-varying current profile. They provide a relatively more accurate estimate of the quantities in question than corresponding asymptotic forms (21) and (23) based on surface current U_s when compared to "exact" values obtained analytically or numerically, as shown for the analytic example of a current with constant shear in section 4, and for the strongly sheared profile of Wu & Tsanis (1995) in section 7.1.

We have further extended the suggestion of BKD17 to represent current information using a Taylor expansion around the peak wavenumber in a modeled spectrum, with extensions covering the specification of action, flux and intrinsic frequency as well as an extension to a general 2D horizontal setting. These results provide an avenue for calculating wave action and action flux in spectral wave models, using a compact set of information about the current field evaluated at the spectral peak wavenumber. The coupling would require that the wave model accept the values $\tilde{\mathbf{U}}, \hat{\mathbf{U}}$ and $\hat{\mathbf{U}}_{,k}$ at each grid point, and corresponding changes would need to be made to the specification of action density and group velocity as a function of frequency and direction within the wave model formulation. These are not huge changes, and hopefully can be implemented in the near future. The corresponding effects on model source terms, such as the representation of nonlinear interactions, is still an open area for research.

Appendix A. Scaling and perturbation solution for the strong current, weak shear case

The theoretical development in KC89 and BKD17 is based on a framework that assumes that the steady current is small compared to wave phase speed, with current shear and profile curvature comparably small. Here, we provide a scaling analysis and perturbation solution that generalizes the problem to the case of a strong depth-uniform current component and arbitrary current orientation in horizontal coordinates, but with deviations from depth-uniformity assumed to be weak. Conceptually, the approach is to write the mean current vector $\mathbf{U}(z)$ as $\mathbf{U}_0 + \mathbf{U}_1(z)$, where the second component carries the information about weak shear and rotation over depth. We do not make an *a priori* choice of how to make this split into two components, and, as will be seen below, the solution itself suggests that $\mathbf{U}_1$ be chosen so as to have a weighted depth-average value of 0 when weighted according to the KC89 procedure.

To develop the non-dimensional form of (4a) - (4c), we introduce the scales ω_0 for frequency or inverse time, k_0 for wavenumber or inverse horizontal distance, and scale vertical coordinate z by uniform depth h. Vertical velocity is scaled by its value at the free surface (determined by the kinematic boundary condition) as

$$w(z) = -i\sigma_s a f(z) \tag{A.1}$$

where σ_s is intrinsic frequency at $z = 0$, a is surface wave amplitude, and $f(z)$ is a dimensionless shape function. Intrinsic frequency σ is given by

$$\begin{aligned} \sigma(z) &= \omega - \mathbf{k}\cdot\mathbf{U}(z) = \omega - \mathbf{k}\cdot\mathbf{U}_0 - \mathbf{k}\cdot\mathbf{U}_1(z) \\ &= \sigma_0 + \sigma_1(z) \end{aligned} \tag{A.2}$$

We define a reference phase speed $c_0 = \omega_0/k_0$ and use $c_0 = \sqrt{gh}$, which fixes the relationship between ω_0 and k_0. For the monochromatic case studied here, we identify ω_0 with ω. Finally, we scale strong depth uniform current $\mathbf{U}_0$ by U and weak current $\mathbf{U}_1$ by $h\Omega$, where Ω represents the strength of current shear or rotation over depth. Referring to (4a) - (4c), we introduce dimensionless parameters $\sigma' = \sigma/\omega_0$ and $k' = k/k_0$. The resulting dimensionless problem (with primes dropped) is then given by

$$\begin{aligned} \sigma(z)(f_{,zz} - k^2\mu^2 f) &= \epsilon\sigma_{1,zz} f; \quad -1 \le z \le 0 \\ \sigma_s^2 f_{,z}(0) &= k^2 + \epsilon\sigma_s\sigma_{1,z}(0) \\ f(0) &= 1; \quad f(-1) = 0 \end{aligned} \tag{A.3}$$

with

$$\sigma(z) = \sigma_0 + \epsilon\sigma_1(z) = (1 - F\mathbf{k}\cdot\mathbf{U}_0) + \epsilon(-\mathbf{k}\cdot\mathbf{U}_1(z)) \tag{A.4}$$

Dimensionless parameters are $\mu = k_0 h = O(1), F = U/c_0 = O(1)$, and $\epsilon = \mu\Omega/\omega_0 \ll 1$, where μ is the usual dispersion parameter resulting from scaling depth by h and horizontal distance by k_0^{-1}, F is a Froude number, and $\epsilon \ll 1$ is a small parameter characterizing current shear. (The alternate approach employed by Ellingsen & Li (2017), where shear is allowed to be strong but curvature weak, would employ the regime $F, \epsilon = O(1)$, with a new small parameter required to characterize the weak curvature.)

Following KC89, we next solve the system (A.3) using a regular perturbation expansion

$$f(z) = \sum_{n=0}^{N} \epsilon^n f_n(z). \tag{A.5}$$

with $f_n(-1) = 0$. In contrast to KC89, we take $f_0(0) = 1$ to satisfy the entire surface boundary condition for f, giving homogeneous conditions $f_n(0) = 0$ for $n > 0$. Introducing (A.4) and (A.5) in (A.3) and sorting by powers of ϵ

gives the governing equations and surface boundary conditions

$$\sigma_0 \left(f_{n,zz} - k^2 \mu^2 f_n \right) = H_n(z) \tag{A.6}$$

$$\sigma_0^2 f_{n,z}(0) = S_n \tag{A.7}$$

At $n = 0$, we have $H_0 = 0$, $S_0 = 1$, and we get the solution

$$f_0(z) = \frac{\sinh \mu k(1+z)}{\sinh \mu k} \tag{A.8}$$

with

$$\sigma_0^2 = \frac{k \tanh \mu k}{\mu} \tag{A.9}$$

which is the usual solution for waves on a depth uniform current. For higher orders $n \geq 1$, use of Green's law for f_0 and f_n leads to a solvability condition

$$\int_{-1}^{0} f_0 H_n dz = S_n \tag{A.10}$$

At $n = 1$, the leading order at which current shear has an effect, we have

$$H_1(z) = \frac{\sigma_{1,zz}}{\sigma_0} f_0(z); \qquad S_1 = \frac{\sigma_{1,z}(0)}{\sigma_0} - \frac{2k^2 \sigma_1(0)}{\sigma_0^3} \tag{A.11}$$

Using (A.11) in (A.10) leads, after cancellations, to the identity

$$\int_{-1}^{0} \sigma_1(z) \cosh 2\mu k(1+z) dz = -\mathbf{k} \cdot \int_{-1}^{0} \mathbf{U}_1(z) \cosh 2\mu k(1+z) dz = 0 \tag{A.12}$$

But $\mathbf{U}_1 = (\mathbf{U} - \mathbf{U}_0)/\epsilon$, which, when substituted in (A.12), gives the result

$$\mathbf{U}_0 = \tilde{\mathbf{U}} = \frac{2\mu k}{\sinh 2\mu k} \int_{-1}^{0} \mathbf{U}(z) \cosh 2\mu k(1+z) dz \tag{A.13}$$

where $\tilde{\mathbf{U}}$ is the depth-weighted current from KC89, extended to allow for $F = O(1)$ and arbitrary direction relative to the wave direction. We thus have the leading order expression for intrinsic frequency $\sigma_0 = \tilde{\sigma} = 1 - F\mathbf{k}\cdot\tilde{\mathbf{U}}$, with leading order dispersion relation

$$\tilde{\sigma}^2 = \frac{k \tanh \mu k}{\mu} \tag{A.14}$$

The expression for phase speed $\mathbf{c}_a$ in a fixed frame is given by

$$\mathbf{c}_a = \frac{\omega}{\mathbf{k}} = \frac{\tilde{\sigma}}{\mathbf{k}} + \tilde{\mathbf{U}} + O(\epsilon^2) \tag{A.15}$$

with no further correction to phase speed at $O(\epsilon)$. Equations (A.6) - (A.7) may then be solved for $f_1(z)$ following the procedure in KC89, giving the result

$$\begin{aligned} f_1(z) \quad = \quad & \left[A_1 + \frac{1}{\mu k} \int_{-1}^{z} H_1(\xi) f_{0,\xi}(\xi)\, d\xi \right] f_0(z) \\ & + \left[B_1 - \frac{1}{\mu k} \int_{-1}^{z} H_1(\xi) f_0(\xi)\, d\xi \right] f_{0,z}(z) \end{aligned} \tag{A.16}$$

with the coefficients A_1 and B_1 of the homogeneous solution resolved by applying the boundary conditions $f_1(0) = f_1(-1) = 0$. Dimensional forms of the results are given in Section 3.1.

Appendix B. Approximations for weak current shear

Starting with the expressions (9a) and (9b) for action density and flux, we develop expansions in powers of ϵ consistent with the approach in Appendix A. In (9a) and (9b), explicit appearances of σ_s and $\mathbf{U}_s$ occur due to the satisfaction of the surface boundary condition and the transformation (7). We assume these should be common to all versions of the expansion that follows. Subsequently, we express $f(z)$ as in (A.5) and use (14) and (16). We then introduce an arbitrary version of the depth uniform current and resulting intrinsic frequency, $\mathbf{U}_0$ and σ_0, as representations of the leading order solution,

$$\mathbf{U}(z) = \mathbf{U}_0 + \epsilon \mathbf{U}_1(z)$$
$$\sigma(z) = \sigma_0 + \epsilon \sigma_1(z) \tag{B.1}$$

where $\sigma_0 = \omega - \mathbf{k} \cdot \mathbf{U}_0$ and $\sigma_1 = -\mathbf{k} \cdot \mathbf{U}_1 = -\mathbf{k} \cdot (\mathbf{U} - \mathbf{U}_0)$, and with associated dispersion relation

$$\sigma_0^2 = gk \tanh kh \tag{B.2}$$

After some simplification of the resulting forms of $\mathcal{N}$ and $\boldsymbol{\mathcal{F}}$, we obtain approximate forms consistent with the present derivation through the choice $\mathbf{U}_0 = \tilde{\mathbf{U}}$ and $\sigma_0 = \tilde{\sigma}$. We also develop an alternate version based on the choice $\mathbf{U}_0 = \mathbf{U}_s$ and $\sigma_0 = \sigma_s$, which leads to expressions for action and flux defined in terms of surface variables, as in Quinn *et al.* (2017). It was our initial expectation that this procedure should reproduce the results in Quinn *et al.* (2017), which are described as being based on the approximate wave-current formulation here and in KC89, but we have not been able to reproduce the results given by Quinn *et al.* (2017), as discussed in Section 7.1.

Substituting the expressions (B.1) and the expansion for $f(z)$ into the formulae (9a) and (9b) and retaining terms to $O(\epsilon)$ leads to the generic version of the expansion, where any remaining occurrences of frequency or current are expressed in terms of σ_0 and $\mathbf{U}_0$. During this process, expressions occurring in terms of $O(\epsilon)$ may be manipulated by choosing $\sigma_0 = \sigma_s$ or $\tilde{\sigma}$ freely, since transformations between these quantities would occur at $O(\epsilon^2)$. In contrast, occurrences of σ_0 in $O(1)$ terms must retain the implied ambiguity, as it's resolution would occur within the accuracy of the approximation.

Proceeding with (9a) for the action density, we note that the integral term is of $O(\epsilon)$, since $\sigma'' = \epsilon\sigma_1''$ for any choice of reference frame. Recognizing that $\sigma_s/\sigma_0 = 1 + O(\epsilon)$ for any choice of reference frame making σ_1 small, we obtain the approximate expression

$$\mathcal{N} = \frac{E_0}{\sigma_s}\left[1 + \epsilon\frac{\sigma_s}{2gk^2}\left(\sigma_{1,z}(0) - \int_{-h}^{0}\sigma_{1,zz}f_0^2 dz\right)\right] + O(\epsilon^2) \tag{B.3}$$

The expression in the interior parentheses may be integrated immediately, and we obtain the approximation

$$\mathcal{N}_0 = \frac{E_0}{\sigma_s}\left[1 + \epsilon\frac{\sigma_s}{\sigma_0^2}(\sigma_s - \tilde{\sigma})\right] + O(\epsilon^2) \tag{B.4}$$

where the single appearance of σ_0 results from a resolution of the combination $gk \tanh kh$.

Turning to the expression for action flux (9b), we note that the first integral term involving f^2 occurs at leading order, and thus the ambiguity of the value of σ_0 must be retained there. We proceed as before by substituting the expansions (B.1). The expression $A(z)$ may be expanded as $\mathbf{A} = \mathbf{A}_0 + \epsilon \mathbf{A}_1 + O(\epsilon^2)$, and we find that $\mathbf{A}_0 = 0$ and

$$\mathbf{A}_1(z) = \sigma_0 \mathbf{U}_{1,z} - \mathbf{U}_0 \sigma_{1,z} \tag{B.5}$$

so that the integral involving $\mathbf{A}_{,z}$ is reduced to

$$\sigma_s^2 \int_{-h}^{0} \sigma^{-2} \mathbf{A}_{,z} f^2 dz = \epsilon \frac{\sigma_s^2}{\sigma_s^2 + O(\epsilon)} \int_{-h}^{0} \mathbf{A}_{1,z} f_0^2 dz + O(\epsilon^2) \tag{B.6}$$

The entire bracketed expression involving $\mathbf{A}$ in (9b) is then evaluated as

$$\epsilon \left[-\mathbf{A}_1(0) + \int_{-h}^{0} \mathbf{A}_{1,z} f_0^2 dz \right] = -\epsilon \frac{k}{\sinh^2 kh} \mathbf{I}_3 \tag{B.7}$$

where

$$\mathbf{I}_3 = \int_{-h}^{0} \mathbf{A}_1(z) \sinh 2k(h+z) dz \tag{B.8}$$

The integral of f^2 is expanded to give

$$\int_{-h}^{0} f^2 dz = I_4 + 2\epsilon I_5 + O(\epsilon^2) \tag{B.9}$$

with

$$I_4 = \int_{-h}^{0} f_0^2 dz; \qquad I_5 = \int_{-h}^{0} f_0 f_1 dz \tag{B.10}$$

and with f_1 given by (16). The resulting expression for the approximation $\boldsymbol{\mathcal{F}}_0$ is then

$$\boldsymbol{\mathcal{F}}_0 = \frac{E_0}{\sigma_s}\left[\mathbf{U}_s + \mathbf{c}_{rs}\left(1 - \frac{\sigma_s^2}{g} I_4\right)\right] - \epsilon\frac{E_0}{\sigma_s}\left[\mathbf{c}_{rs}\frac{2\sigma_s^2}{g} I_5 + \frac{\sigma_s}{\sigma_0^2 \sinh 2kh}\mathbf{I}_3\right] \tag{B.11}$$

Integrals $\mathbf{I}_3$ and I_4 are given to the required order by

$$\begin{aligned} \mathbf{I_3} &= \sinh 2kh\left[\sigma_0(\mathbf{U}_s - \tilde{\mathbf{U}}) + \mathbf{U}_0(\tilde{\sigma} - \sigma_s)\right] \\ I_4 &= \frac{g}{2\sigma_0^2}(1 - G); \qquad G = \frac{2kh}{\sinh 2kh} \end{aligned} \tag{B.12}$$

The expression for I_5 is complex, and is given after some initial effort by

$$I_5 = \frac{1}{4\tilde{\sigma}\sinh^2 kh}\left[\frac{G\cosh^2 kh}{k} I_2(0) - I_6\right] \tag{B.13}$$

where (from (17))

$$I_2(0) = 2\sinh^2 kh(\hat{\mathbf{k}} \cdot \mathbf{U}_{,z}(0)) + 2\sinh 2kh(\sigma_s - \tilde{\sigma}) \tag{B.14}$$

and

$$I_6 = \int_{-h}^{0} \hat{\mathbf{k}} \cdot \mathbf{U}_{,zz}(z)(h+z)\sinh 2k(h+z)dz \tag{B.15}$$

An expression for I_6 is obtained by first expressing $\tilde{\mathbf{U}}$ in terms of $\mathbf{U}_{,zz}$ using two integrations by parts, differentiating the resulting expression with respect to wavenumber k, and taking the dot product with the unit wavenumber $\hat{\mathbf{k}}$ to obtain (after rearrangement)

$$I_6 = \sinh 2kh \left[\mathbf{k} \cdot \tilde{\mathbf{U}}_{,k} + h\hat{\mathbf{k}} \cdot \mathbf{U}_{1,z}(0) + \frac{1}{k} \big((1-G) + 2G\cosh^2 kh \big) (\sigma_s - \tilde{\sigma}) \right] \tag{B.16}$$

Using (B.14) and (B.16) in (B.13) leads to a relatively compact expression for I_5 given by

$$I_5 = -\frac{1}{2\tilde{\sigma}\tanh kh} \left[\mathbf{k} \cdot \tilde{\mathbf{U}}_{,k} + \frac{1}{k}(1-G)(\sigma_s - \tilde{\sigma}) \right] \tag{B.17}$$

Using the results for $\mathbf{I}_3, I_4$ and I_5 in (B.11) leads finally to

$$\begin{aligned} \boldsymbol{\mathcal{F}}_0 &= \frac{E_0}{\sigma_s} \left[\mathbf{U}_s + \mathbf{c}_{rs} \left(1 - \frac{1}{2} \left(\frac{\sigma_s}{\sigma_0} \right)^2 (1-G) \right) \right] \\ &\quad + \epsilon \frac{E_0}{\sigma_s} \left[\frac{\sigma_s^3 \hat{\mathbf{k}}}{\tilde{\sigma}\sigma_0^2} \left(\mathbf{k} \cdot \tilde{\mathbf{U}}_{,k} + \frac{1}{k}(1-G)(\sigma_s - \tilde{\sigma}) \right) \right. \\ &\quad \left. - \frac{\sigma_s}{\sigma_0^2} \left(\sigma_0 (\mathbf{U}_s - \tilde{\mathbf{U}}) + (\tilde{\sigma} - \sigma_s) \mathbf{U}_0 \right) \right] \end{aligned} \tag{B.18}$$

From this point, the resolution of the expressions for $\mathcal{N}_0$ and $\boldsymbol{\mathcal{F}}_0$ involves the choice of σ_0. Following the procedure of referencing all quantities to surface conditions leads to an expression for $\mathcal{N}_0$ given by

$$\mathcal{N}^* = \mathcal{N}_0(\sigma_s) = \frac{E_0}{\sigma_s} \left[1 + \epsilon \frac{(\sigma_s - \tilde{\sigma})}{\sigma_s} \right] + O(\epsilon^2) \tag{B.19}$$

This result is similar in form to that in Quinn *et al.* (2017), equation (4.2), but there is no clear relation between the residual $O(\epsilon)$ terms in the two results, as discussed further in Section 7.1.

Taking the alternate approach of referencing quantities to the frame moving with speed $\tilde{\mathbf{U}}$ leads to the expression

$$\tilde{\mathcal{N}} = \mathcal{N}_0(\tilde{\sigma}) = \frac{E_0}{\tilde{\sigma}} + O(\epsilon^2) \tag{B.20}$$

where all information about the approximation within the order of accuracy is contained in the simple ratio of E_0 and $\tilde{\sigma}$.

The same process applied to $\boldsymbol{\mathcal{F}}_0$ in (B.18) leads to the expressions

$$\boldsymbol{\mathcal{F}}^* = \frac{E_0}{\sigma_s}\left[\hat{\mathbf{U}} + \mathbf{c}_{grs} + \epsilon\left(\mathbf{U}_s\left(\frac{\sigma_s - \tilde{\sigma}}{\sigma_s}\right) + \frac{\hat{\mathbf{k}}}{k}(1-G)(\sigma_s - \tilde{\sigma})\right)\right] + O(\epsilon^2) \tag{B.21}$$

and

$$\tilde{\boldsymbol{\mathcal{F}}} = \frac{E_0}{\tilde{\sigma}}\left[\hat{\mathbf{U}} + \tilde{\mathbf{c}}_{gr}\right] + O(\epsilon^2) \tag{B.22}$$

where $\mathbf{c}_{grs}$ and $\tilde{\mathbf{c}}_{gr}$ are relative group velocities (defined in the usual sense for a depth uniform current) relative to the surface and depth weighted velocities respectively.

Acknowledgments: This work was supported by grants OCE-1334325, OCE-1435147 and OCE-1756355 from the Physical Oceanography Program, National Science Foundation. Computational resources were provided by Instructional Technology, University of Delaware.

Ardhuin, F., Rascle, N. & Belibassakis, K. A. 2008 Explicit wave-averaged primitive equations using a generalized Lagrangian mean. *Ocean Modelling* **20**, 35–60.

Banihashemi, S., Kirby, J. T. & Dong, Z. 2017 Approximation of wave action flux velocity in strongly sheared mean flows. *Ocean Modelling* **116**, 33–47.

BOOIJ, N., RIS, R. C. & HOLTHUIJSEN, L. H 1999 A third-generation wave model for coastal regions: 1. model description and validation. *J. Geophys. Res: Oceans* **104** (C4), 7649–7666.

BRETHERTON, F. P. & GARRETT, C. J. R. 1968 Wavetrains in inhomogeneous moving media. *Proc. of R. Soc. London* **302**, 529–554.

CRAIK, A. D. D. 1968 Resonant gravity-wave interactions in a shear flow. *Journal of Fluid Mechanics* **34** (3), 531–549.

DINGEMANS, M. W. 1997 *Water Wave Propagation over Uneven Bottoms. Part I: Linear Wave Propagation*. World Scientific.

DONG, Z. & KIRBY, J. T. 2012 Theoretical and numerical study of wave-current interaction in strongly-sheared flows. In *Proc. 33d Int. Conf. Coastal Eng.* (ed. P. Lynett & J. M. Smith). Santander, Spain.

ELIAS, E. P. L., GELFENBAUM, G. & VAN DER WESTHUYSEN, A. J. 2012 Validation of a coupled wave-flow model in a high-energy setting: The mouth of the Columbia River. *J. Geophys. Res* **117**, C09011, doi:10.1029/2012JC008105.

ELLINGSEN, S. A. 2016 Oblique waves on a vertically sheared current are rotational. *European J. of Mechanics B/Fluids* **56**, 156–160.

ELLINGSEN, S. A. & LI, Y. 2017 Approximate dispersion relations for waves on arbitrary shear flows. *Journal of Geophysical Research: Oceans* **122**, 9889–9905.

Fenton, J. D. 1973 Some results for surface gravity waves on shear flows. *J. Inst. Math. Appl.* **12** (1), 1–20.

Hasselmann, K., et al. 1973 Measurements of wind-wave growth and swell decay during the Joint North Sea Wave Project (JONSWAP). *Ergänzungsheft 8-12* .

Jonsson, Ivar G 1990 Wave-current interactions. *The Sea: Ocean Engineering Science* **9**, 65–119.

Jonsson, I. G., Brink-Kjaer, O. & Thomas, G. P. 1978 Wave action and set-down for waves on a shear current. *J. Fluid Mech.* **87**, 401–416.

Kilcher, L. F. & Nash, J. D. 2010 Structure and dynamics of the Columbia River tidal plume front. *J. Geophys. Res.* **115**, C05S90, doi:10.1029/2009JC006066.

Kirby, J. T & Chen, T. 1989 Surface waves on vertically sheared flows: approximate dispersion relations. *J. Geophys. Res.* **94**, 1013–1027.

Li, Y. & Ellingsen, S. A. 2019 A framework for analysing surface waves on arbitrary shear currents in constant and varying water depth. *Journal of Geophysical Research: Oceans* **124**, 2527–2545.

Peregrine, D. H. 1976 Interaction of water waves and currents. *Adv. Appl. Mech.* **16**, 9–117.

Quinn, B. E., Toledo, Y. & Shrira, V. I. 2017 Explicit wave action conservation for water waves on vertically sheared flows. *Ocean Modelling* **112**, 33–47.

SHRIRA, V. I. 1993 Surface waves on shear currents: solution of the boundary-value problem. *J. Fluid Mechanics* **252**, 565–584.

SKOP, R. A 1987 Approximate dispersion relation for wave-current interactions. *J. Waterway, Port, Coastal, and Ocean Eng.* **113**, 187–195.

STEWART, R. H. & JOY, J. W. 1974 Hf radio measurements of surface currents. *Deep Sea Research and Oceanographic Abstracts* **21**, 1039–1049.

THOMAS, G.P. & KLOPMAN, G. 1997 Wave-current interactions in the near shore region. *Int. Series on Advances in Fluid Mechanics* **10**, 255–319.

THOMPSON, P. D. 1949 The propagation of small surface disturbances through rotational flow. *Annals of the New York Academy of Sciences* **51**, 463–474.

VORONOVICH, A. G. 1976 Propagation of internal and surface gravity waves in the approximation of geometrical optics. *Izvestia Atmospheric and Oceanic Physics* **12**, 850–857.

VAN DER WESTHUYSEN, A. & LESSER, G. 2007 Evaluation and development of wave-current interaction in SWAN: activity 6.4 of SBW project Waddenzee. *Tech. Rep.*. Deltares (WL).

WHITHAM, G. B. 1974 *Linear and Nonlinear Waves*. John Wiley , New York.

WU, J. & TSANIS, I. K. 1995 Numerical study of wind-induced water currents. *Journal of Hydraulic Engineering* **121** (5), 388–395.

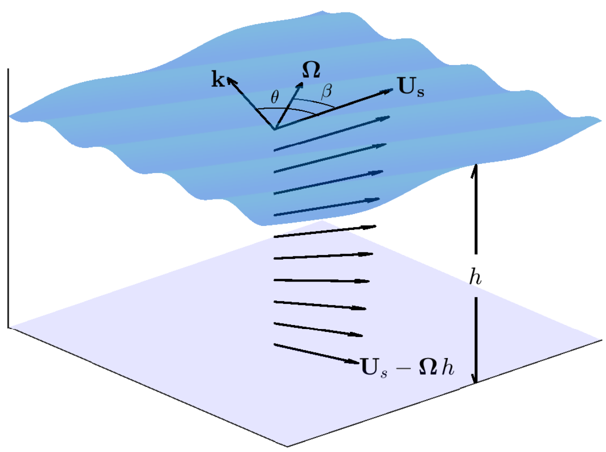

Figure 1: Definition sketch for linear shear current. The angle between the surface velocity and wave direction is θ while the angle between the surface current and current vertical shear is β

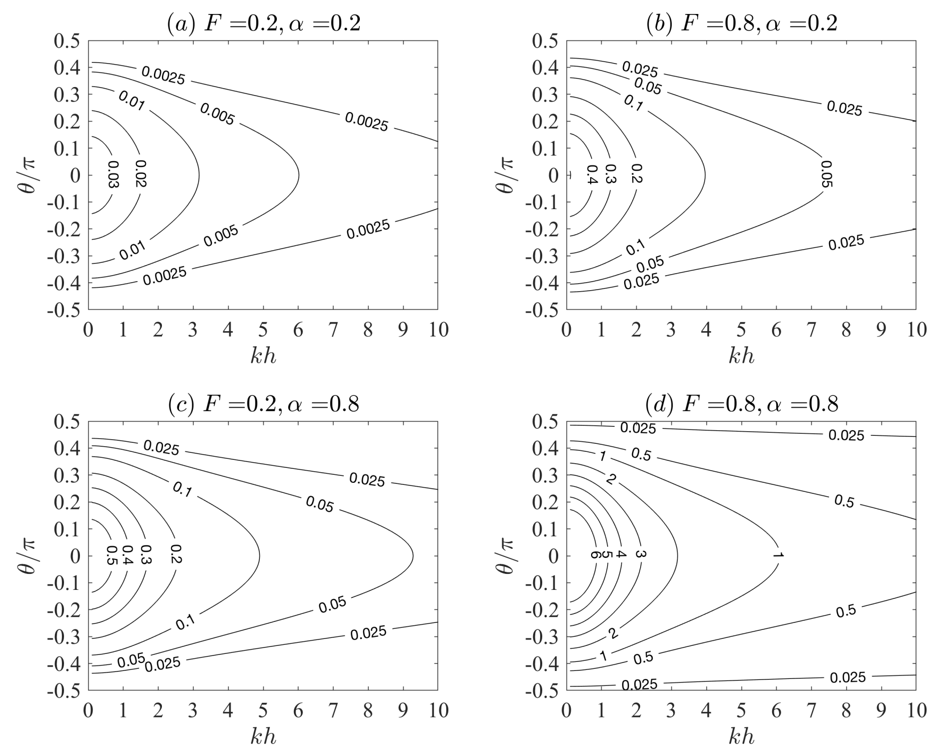

Figure 2: % error in wave action density $100(1-\tilde{\mathcal{N}}/\mathcal{N})$: linear shear with variation of kh and θ, first order perturbation approximation, $\beta = 0$.

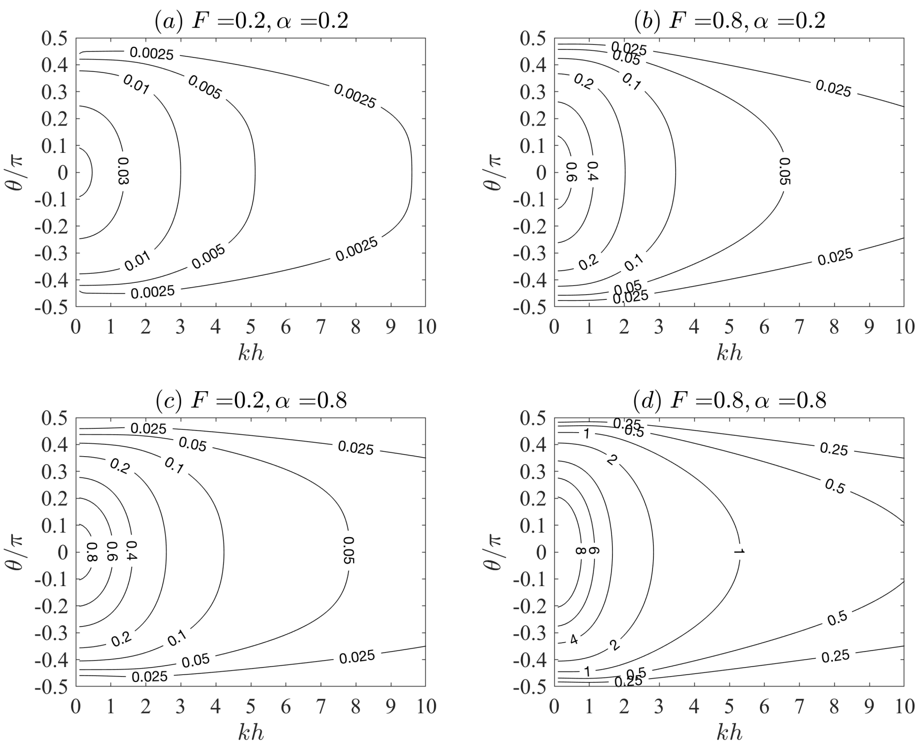

Figure 3: % error in wave action flux $100(1 - |\tilde{\boldsymbol{\mathcal{F}}}|/|\boldsymbol{\mathcal{F}}|)$: linear shear with variation of kh and θ, first order perturbation approximation, $\beta = 0$.

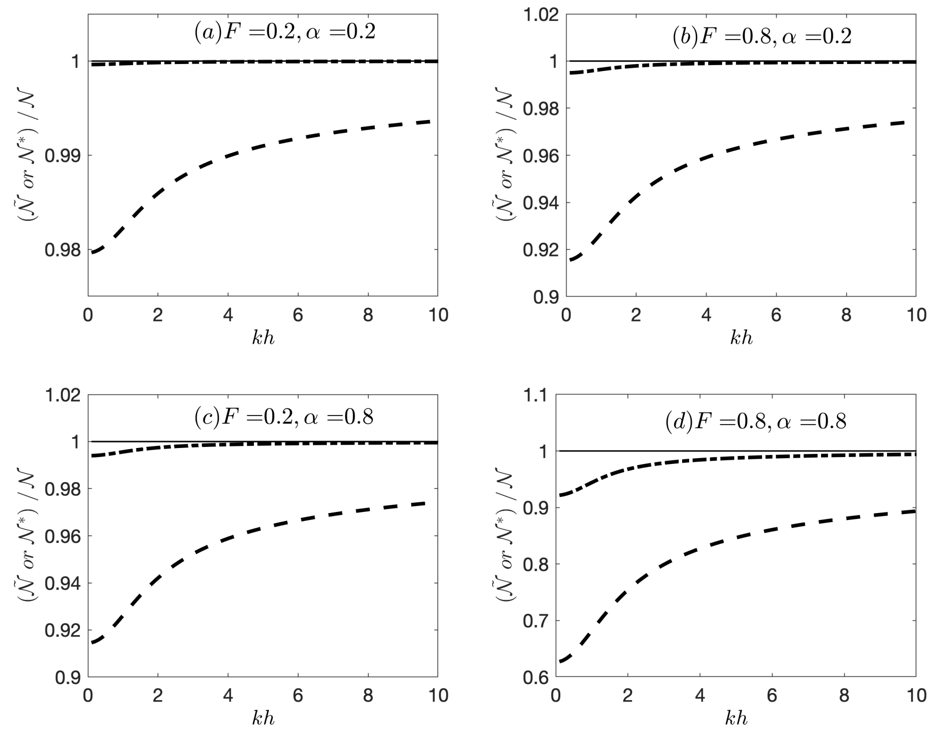

Figure 4: Comparison of action density estimates: linear shear with variation of kh, with $\theta = 0$ and $\beta = 0$. Dashed dotted lines indicate $\tilde{\mathcal{N}}/\mathcal{N}$ using the asymptotic expression (21) in the frame of reference based on the depth weighted current, dashed lines indicate $\mathcal{N}^*/\mathcal{N}$ using the asymptotic expression (20) in the frame of reference based on the surface current.

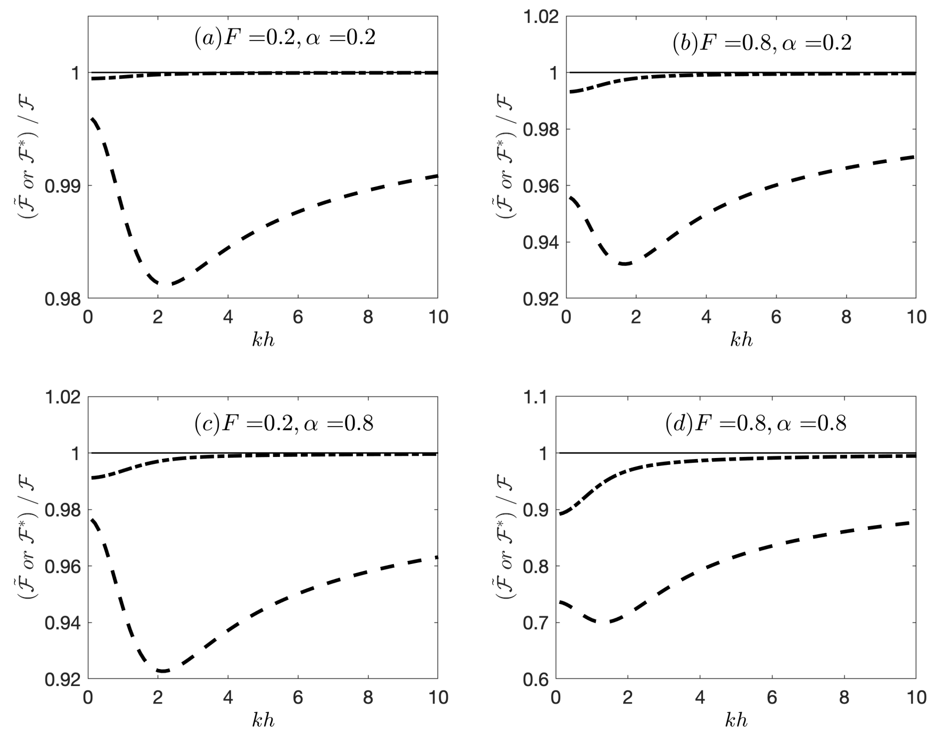

Figure 5: Comparison of action flux: linear shear with variation of kh with $\theta = 0$ and $\beta = 0$. Dashed dotted lines indicate $\tilde{\boldsymbol{\mathcal{F}}}/\boldsymbol{\mathcal{F}}$ using the asymptotic expression (23) in the frame of reference based on the depth weighted current, dashed lines indicate $\boldsymbol{\mathcal{F}}^*/\boldsymbol{\mathcal{F}}$ using the asymptotic expression (22) in the frame of reference based on the surface current.

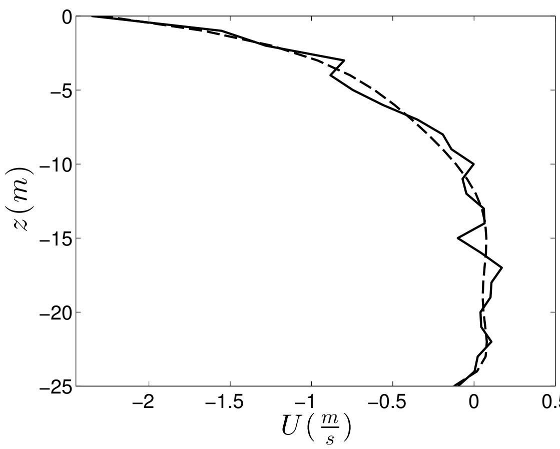

Figure 6: Columbia River current profile during ebb tide. The solid line is measured data (Kilcher & Nash, 2010) and the dashed line is a 6th order polynomial fit to the data.

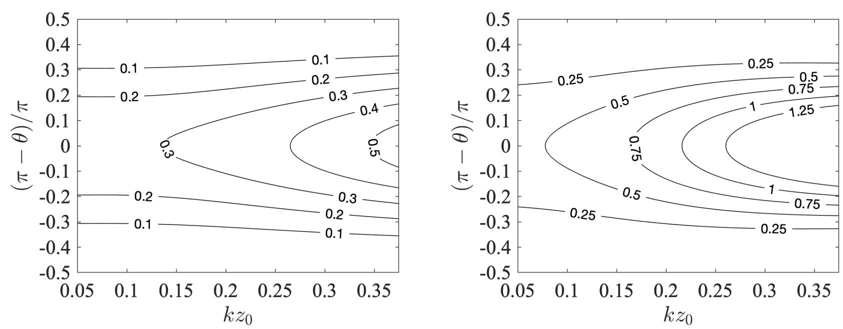

Figure 7: % error in wave action density $100(1 - \tilde{\mathcal{N}}/\mathcal{N})$ (left) and wave action flux $100(1 - |\tilde{\boldsymbol{\mathcal{F}}}|/|\boldsymbol{\mathcal{F}}|)$ (right): MCR current profile with variation of kz_0 and θ, first order perturbation approximations (21) and (23).

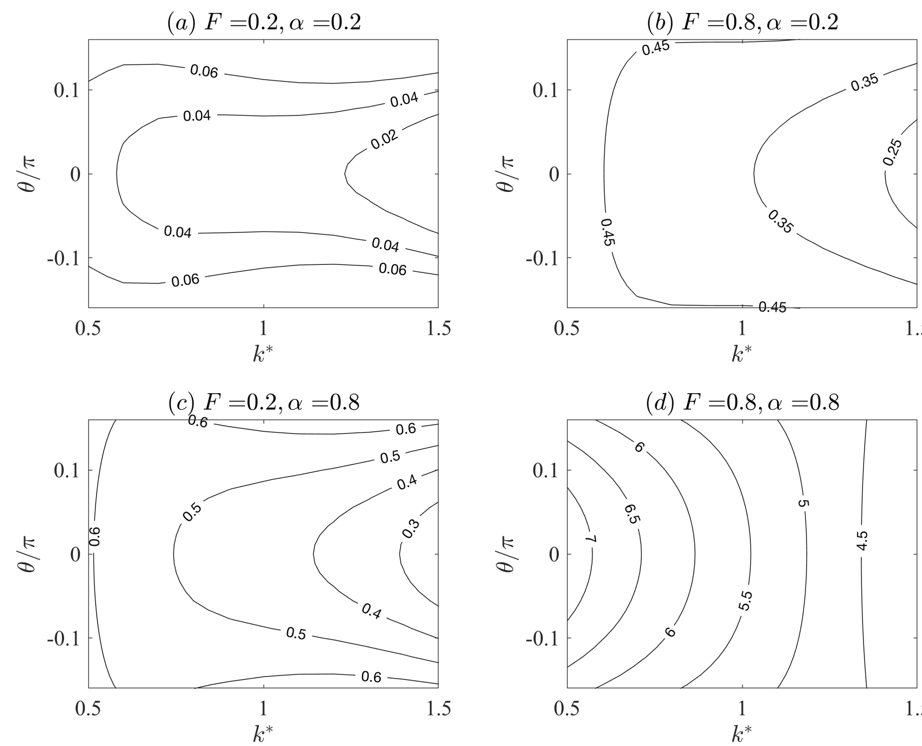

Figure 8: % error $100(1-\tilde{\mathcal{N}}_T/\mathcal{N})$ in wave action density $\tilde{\mathcal{N}}_T$ for the Taylor series expansion about the peak wavenumber $\mathbf{k}^p$ with $k^* = k/k^p$: Constant shear current, $k^p h = 1$, $\beta = 0$.

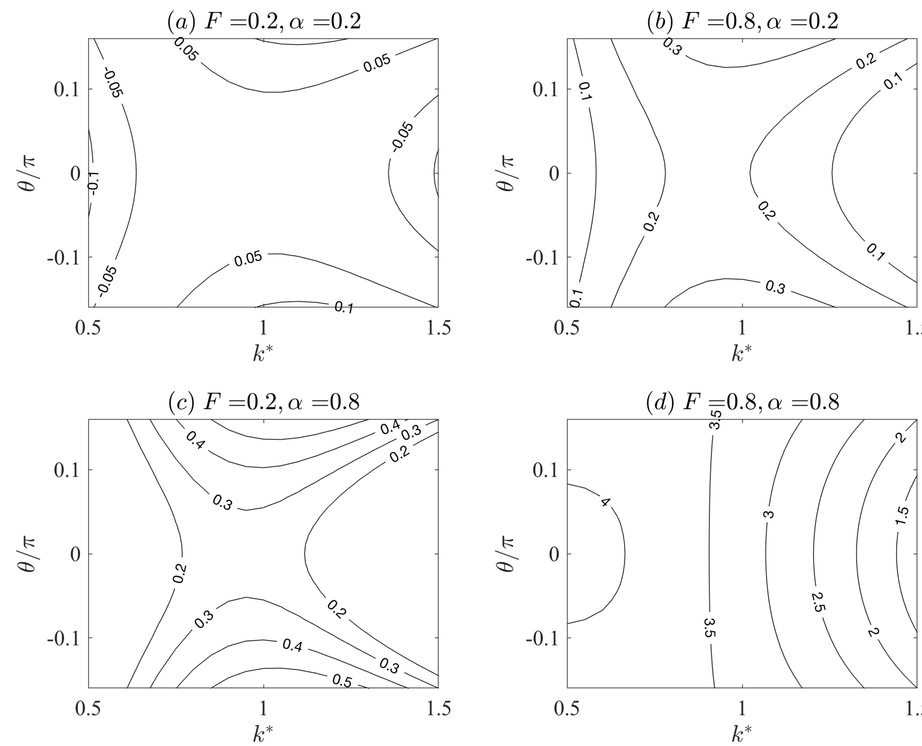

Figure 9: As in Figure 8: Constant shear current, $k^p h = 2$, $\beta = 0$.

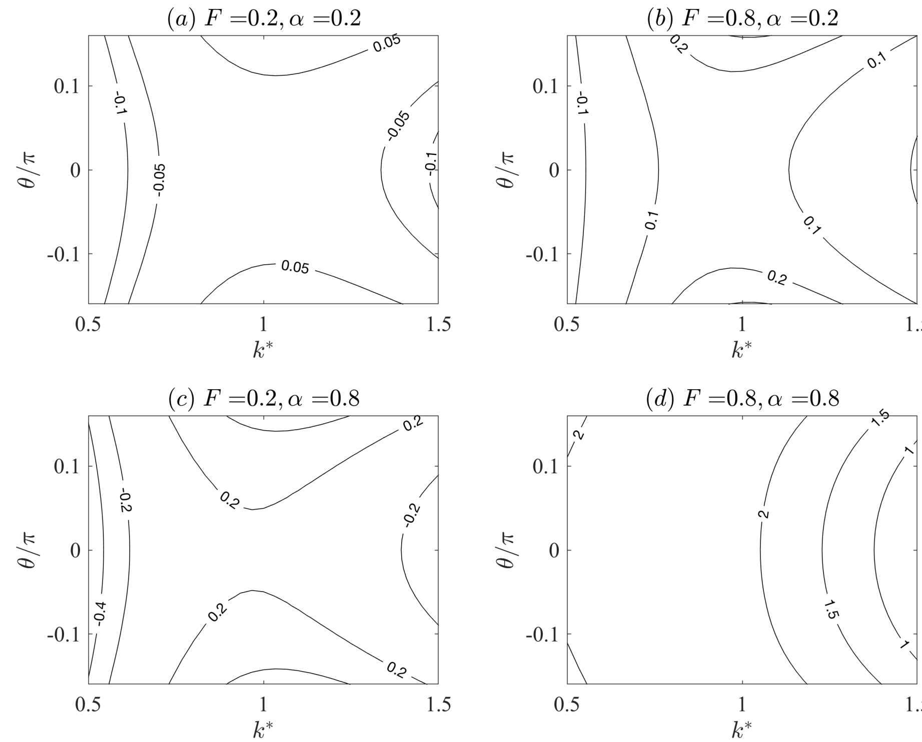

Figure 10: As in Figure 8: Constant shear current, $k^p h = 3$, $\beta = 0$.

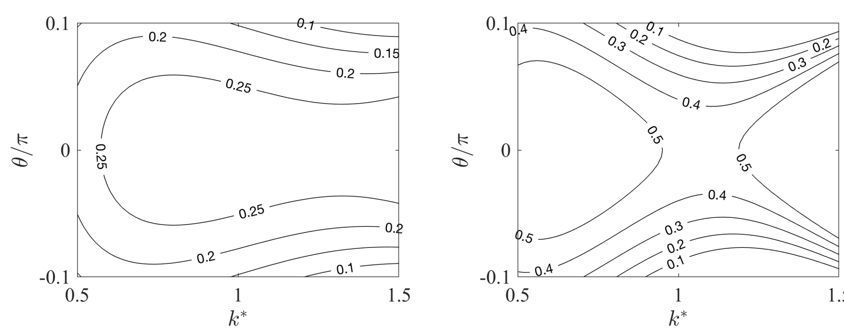

Figure 11: As in Figure 8: MCR current profile, $k^p h = 1$ (left) and $k^p h = 2$ (right), $\beta = 0$.

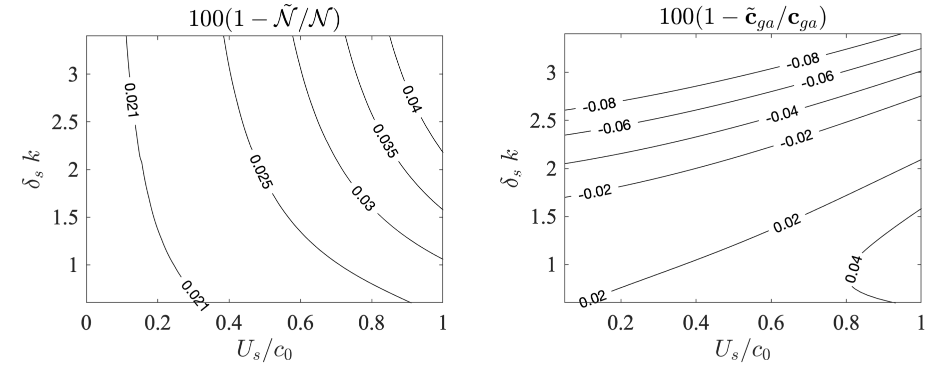

Figure 12: % error in estimates in action density $\tilde{\mathcal{N}}$ (left) and group velocity $\tilde{c}_{ga}$ (right), estimates for the case of Wu & Tsanis (1995) profile using the asymptotic expressions (21) and (23) in the frame of reference based on the depth-weighted current $\tilde{\mathbf{U}}$.

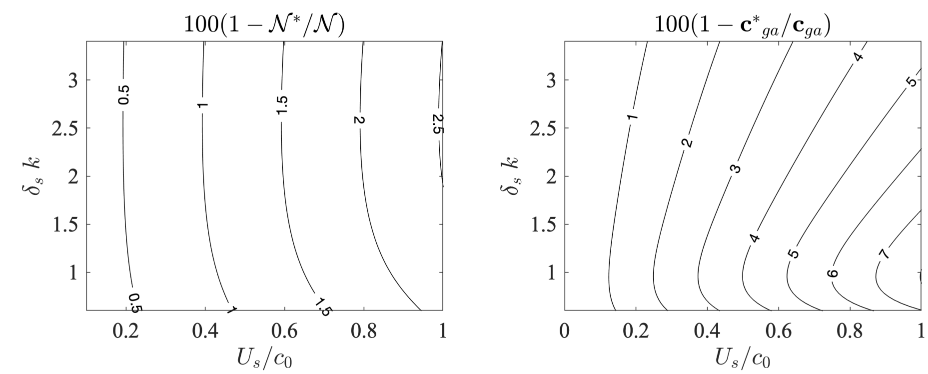

Figure 13: % error in estimates of action density $\mathcal{N}^*$ (left) and group velocity c^*_{ga} (right), estimates for the case of Wu & Tsanis (1995) profile using the asymptotic expressions (20) and (22) in the frame of reference based on the surface current.